Electrical Engineering
https://doi.org/10.1007/s00202-023-02029-5

ORIGINAL PAPER

New methodologies for SVC modeling in the power flow problem based on sigmoid functions

João Pedro Peters Barbosa[1] · João Alberto Passos Filho[1]

Received: 29 April 2023 / Accepted: 6 September 2023

Abstract
This paper presents new methodologies for modeling static VAr compensators (SVCs) in the power flow problem. The proposed formulations utilize sigmoid functions to model the control equations that describe the steady-state behavior of SVCs. The first methodology introduces reactive power injection as a new state variable, while the second methodology utilizes the thyristor firing angle. These steady-state SVC methodologies were applied to the power flow problem using the full Newton formulation, which incorporates the control equations into the system of nonlinear equations. One of the main contributions of these proposed methodologies is that they eliminate the need for alternating adjustments concerning the operational limits of the SVC during the iterative power flow process. The implementation of a power flow program was tested on both small-scale tutorial systems and the medium-scale IEEE Nordic system. The presented results validate and demonstrate the effectiveness of the proposed methodology.

Keywords Static VAr compensator · Power flow · Control devices · Sigmoid functions

1 Introduction

Modern research and operation of electrical power systems heavily rely on power flow as a fundamental analytical tool. Its application provides vital information about bus voltages, active and reactive power flows in system components, as well as reactive power generation for a given load and generation scenario. This analysis, combined with network topology, allows for in-depth studies on various topics of interest such as electrical system operation, planning operation, and planning expansion [1]. Based on these analyses, an important issue for the operation of modern power systems relates to voltage control. Maintaining a consistently regulated voltage magnitude throughout the entire network is crucial for ensuring reliable power system operation. This objective can be achieved by effectively controlling the injection, absorption, and flow of reactive power within the electrical system [2].

Static VAr compensators (SVCs) shall receive a notable mention among the electric devices capable of actively participating in voltage regulation. SVCs are one of the most popular Flexible AC Transmission System (FACTS) devices that, of the multiple benefits it can provide to a network, enhancement of voltage stability margins can be highlighted [3, 4]. Therefore, it is crucially important to develop and implement precise modeling of this device during power flow analysis to achieve results as realistically as possible.

SVCs are the research focus of many works found in the literature. In [3], it evaluated power systems voltage stability improvements in the presence of SVCs. Steady-state model of the SVC for power flow and optimal power flow studies is proposed in [2]. Focusing on optimal power flow, work [5] proposes the implementation of partitioned ant lion algorithm to improve SVC modeling. Additionally, in [6] the SVC operates with wind power generators to enhance voltage compensation. The reference [7] presents an approach to control power systems with several FACTS devices, including SVC. A comparison of an optimal power flow formulation, with and without FACTS devices such as SVC and thyristor-controlled series capacitor (TCSC), in terms of cost saving

João Pedro Peters Barbosa and João Alberto Passos Filho contributed equally to this work

✉ João Alberto Passos Filho
joao.passos@ufjf.br

João Pedro Peters Barbosa
joao.peters@ieee.org

[1] Department of Electrical Energy, Federal University of Juiz de Fora, Rua Jose Lourenco Kelmer, Juiz de Fora, MG 36036-900, Brazil

Published online: 27 September 2023

and loss reduction in a smart grid scenario is presented by [8]. Different methods of bio-inspired optimization techniques are addressed in [9] to find out the most favorable location and firing angle of SVC in power systems.

Considering the complexity of modeling SVC in the nonlinear power flow problem, this paper explores the use of sigmoid functions to introduce new solutions strategies. In terms of considering control limits and saturation effects approximations, the sigmoid function characteristic fits within the requirements of smooth functions for studies related to voltage stability and bifurcations [10–12]. Therefore, traditional control devices methodologies, such as synchronous machines operative limits, HVDC links operative limits, transformer's on-load tap and phase shift controls, and shunt devices compensation control, all can be reformulated considering the implementation of sigmoid functions.

From this context, the main contributions of this work are the following:

- A new methodology to represent SVC in the power flow problem based on the equipment's reactive power injection;
- A new methodology to represent SVCs in the power flow problem based on the thyristor firing angle methodology [2], proposing a *droop* improvement to the model;
- A generic methodology to represent the control devices limits and saturation effects in power systems operation based on sigmoid functions.

The classical methodologies for representing SVC in the power flow problem consider the change of operating region (linear, inductive, and capacitive) by swapping the corresponding equation during the iterative solution process. The problem is that in this case, the evaluation of the operating region is performed alternately with the iterative process, typically using the minimum and maximum voltage values of the linear region as criteria. Thus, one of the main contributions of this work is the proposition of methodologies where the control region alteration is fully automatic and in accordance with the complete Newton method, leading to a more robust numerical process by preserving the quadratic convergence characteristic of the Newton method.

Altogether, a review and a new modeling strategy of the main steady-state SVC methodologies is made. For the proposed methodologies, a full Newton approach is considered, implying on the automatic incorporation of control equations throughout the power flow iterative simulation. In this case, sigmoid function-based switches enable or disable the control equation that best describes SVCs current operational states that will be linearized and incorporated into the Jacobian matrix at each iteration. The proposed methodologies have been tested in a small-scale tutorial system [1] and the well-known IEEE Nordic system [13] and were validated in a Brazilian production-grade software developed by CEPEL (Electric Energy Research Center).

The paper is organized as follows: In Sect. 2 is presented a review of the main representation methodologies for SVCs' reactive power generation in the power flow problem. The proposed methodologies are detailed in Sect. 3. An analysis on the proposed methodologies simulation results is presented in Sect. 4. In conclusion, Sect. 5 summarizes the main results and contributions of the paper. The bold variables presented in this paper are treated as functions or vectors.

2 Background of modeling control devices

The current literature describes two approaches for modeling control devices in the power flow problem using the Newton method as follows:

- The adjusted solution approach, where the power flow solution is adjusted in an alternate manner from iteration to iteration [14, 15];
- The full Newton approach, which allows steady-state equations for each control device to be fully represented into the Jacobian matrix in several ways [16–18].

The latter approach produces a faster and more robust convergence. A flexible representation of control devices is obtained by augmenting the basic Newton power flow formulation, with the steady-state equations describing each control device and the associated controlled variable, generating a system of equations of order (*2nb+nc*), with *nb* being the number of system buses and *nc* the total number of power flow controls. This formulation leads to the following generic augmented Jacobian matrix:

$$\begin{bmatrix} \Delta \boldsymbol{P} \\ \Delta \boldsymbol{Q} \\ \Delta \boldsymbol{y} \end{bmatrix} = \begin{bmatrix} \frac{\mathbf{d}\boldsymbol{P}}{\mathbf{d}\boldsymbol{\theta}} & \frac{\mathbf{d}\boldsymbol{P}}{\mathbf{d}\boldsymbol{V}} & \frac{\mathbf{d}\boldsymbol{P}}{\mathbf{d}\boldsymbol{x}} \\ \frac{\mathbf{d}\boldsymbol{Q}}{\mathbf{d}\boldsymbol{\theta}} & \frac{\mathbf{d}\boldsymbol{Q}}{\mathbf{d}\boldsymbol{V}} & \frac{\mathbf{d}\boldsymbol{Q}}{\mathbf{d}\boldsymbol{x}} \\ \frac{\mathbf{d}\boldsymbol{y}}{\mathbf{d}\boldsymbol{\theta}} & \frac{\mathbf{d}\boldsymbol{y}}{\mathbf{d}\boldsymbol{V}} & \frac{\mathbf{d}\boldsymbol{y}}{\mathbf{d}\boldsymbol{x}} \end{bmatrix} \cdot \begin{bmatrix} \Delta \boldsymbol{\theta} \\ \Delta \boldsymbol{V} \\ \Delta \boldsymbol{x} \end{bmatrix} \tag{1}$$

where

$$\Delta \boldsymbol{P} = \boldsymbol{P}^{\mathbf{sch}} - \boldsymbol{P}^{\mathbf{cal}} \tag{2}$$

$$\Delta \boldsymbol{Q} = \boldsymbol{Q}^{\mathbf{sch}} - \boldsymbol{Q}^{\mathbf{cal}} \tag{3}$$

$$P_k^{\mathrm{cal}}(\boldsymbol{\theta}, \boldsymbol{V}, \boldsymbol{x}) = V_k \cdot \sum_{i \in \Omega_k} V_m \cdot (G_{km} \cdot \cos(\theta_{km}) + B_{km} \cdot \sin(\theta_{km})) \tag{4}$$

$$Q_k^{cal}(\boldsymbol{\theta}, \boldsymbol{V}, \boldsymbol{x}) = V_k \cdot \sum_{i \in \Omega_k} V_m \cdot (G_{km} \cdot \sin(\theta_{km}) - B_{km} \cdot \cos(\theta_{km})) \tag{5}$$

where the symbol Ω_k denotes the set of all buses connected to bus k, including the own bus k. The terms G_{km} and B_{km} are the real and imaginary elements of the nodal admittance matrix, respectively. As indicated in (1), the now incorporated control equations mismatch is given by:

$$\Delta \boldsymbol{y} = \boldsymbol{y}^{\mathbf{sch}} - \boldsymbol{y}^{\mathbf{cal}} \tag{6}$$

and corresponds not only to the expanded state vectors $\Delta\boldsymbol{\theta}$, $\Delta\boldsymbol{V}$ mismatches, but also to the control variables vector $\Delta\boldsymbol{x}$ mismatch. The superscripts sch and cal presented in (2), (3) and (6) denote scheduled and calculated variables.

The incorporation of control equations as shown in (1) determines the way that control variables $\boldsymbol{x}$ change as so to ensure that it reaches their specified values at convergence. The control variables, being now an integral part of the expanded state vector, are updated at every iteration altogether with the state variables, as follows:

$$\begin{aligned} \boldsymbol{\theta}^{(h+1)} &= \boldsymbol{\theta}^{(h)} + \Delta\boldsymbol{\theta}^{(h)} \\ \boldsymbol{V}^{(h+1)} &= \boldsymbol{V}^{(h)} + \Delta\boldsymbol{V}^{(h)} \\ \boldsymbol{x}^{(h+1)} &= \boldsymbol{x}^{(h)} + \Delta\boldsymbol{x}^{(h)} \end{aligned} \tag{7}$$

where the symbol "h" denotes iteration number.

In the basic Newton power flow formulation, the convergence criterion is given in terms of a tolerance for active and reactive power mismatches. With the incorporation of control devices, an additional convergence check is needed; the value of $\| \Delta\boldsymbol{y} \|_\infty$ must be smaller than a tolerance. Hence, a production-grade Newton power flow should be flexible in order to incorporate and remove the control equations that best represent the control device's behavior during the iterative solution process, accurately modeling their operational limits for all loading conditions.

The methodology for representing control devices in the power flow problem, presented in this section, will be used in the following sections to describe the SVC modeling.

3 SVC's traditional methodologies

Hereinafter are detailed the most traditional mathematical models for SVCs. These models, when incorporated into Newton–Raphson's numerical method, contribute to mathematical robustness and control flexibility [1]. Nevertheless, precise operational results not only depend on correct mathematical modeling but also on a correct formulation process [15, 19, 20].

As FACTS devices began to develop due to advances in power electronics technology, the operation of electrical power systems became more reliable and efficient [21]. The SVC integrates FACTS device's family as a shunt-connected variable reactance, which is able to generate or absorb reactive power while connected at a high-voltage alternating current (HVAC) power network bus [22] within a fixed and continuous range. Despite its limited capacity, it offers faster control response and enables quicker reactive power compensation, voltage regulation support, and an enhancement in system stability margin [2–4]. Among the electrical configurations available in the literature, the fixed-capacitor thyristor-controlled reactor (FC-TCR), as shown in Fig. 1, is one of the most commonly adopted in researches and in real-life operations.

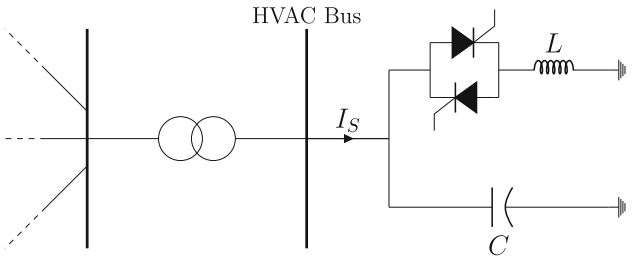

Fig. 1 Static VAr compensator fixed-capacitor thyristor-controlled reactor configuration

A traditional steady-state SVC model was first introduced in [22, 23], treating the control device as a synchronous condenser. The proposed modeling is acceptable for operations within the reactive power generation limits; otherwise, it can lead to inaccurate results. Departing from this consideration and Fig. 1 topology, [2] proposes a new model based on the SVC variable shunt susceptance characteristic and the thyristor firing angle value. Although the aforesaid methodology improves the SVC representation in the power flow problem, a simplification on the control device *droop* is still carried out.

An alternative model based on the control device's characteristic QV-curve is presented, which takes into consideration the SVC *droop* in the linear region of operation and better representing the realistic operation condition of the control device. To detail the differences, the following subsections describe the representations on which each methodology is based.

3.1 SVC's thyristor firing angle methodology

The SVC's thyristor firing angle methodology proposed by [2] is better represented by the set of graphics in Fig. 2. The thyristor firing angle α is taken as the new power flow state variable, varying between its limits ($90° \leq \alpha \leq 180°$) and adjusting the equipment's equivalent reactance and susceptance values in accordance with Eqs. (9) and (10), respectively.

In the proposed methodology, the SVC reactive power generation is calculated via the equivalent susceptance

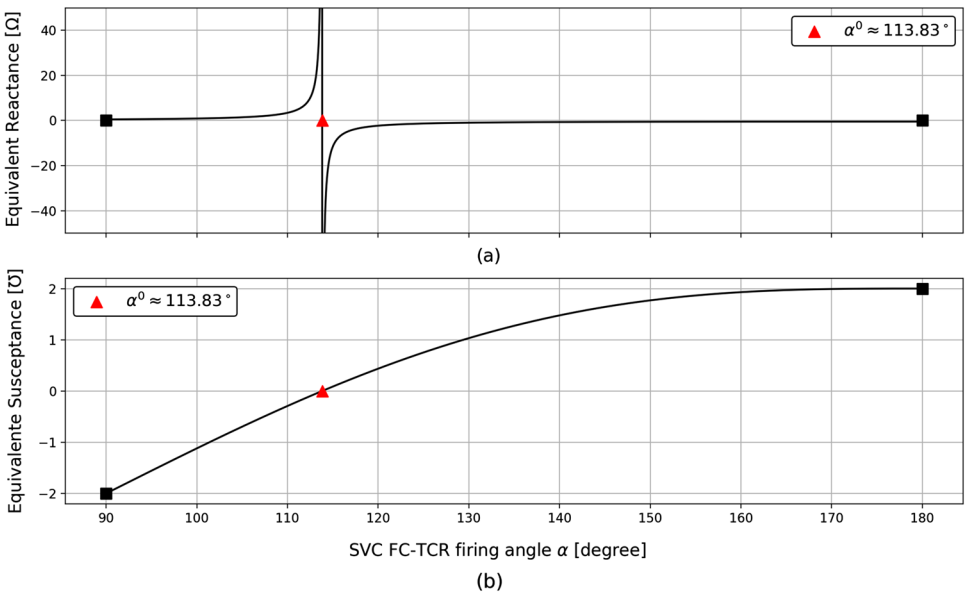

Fig. 2 SVC **a** equivalent reactance and **b** equivalent susceptance as functions of the thyristor firing angle. Adapted from [2]

because its continuity, shown in Fig. 2b, configures a better numerical behavior when linearized into the Jacobian matrix in contrast to the SVC equivalent reactance [2]. Numerically, (9) presents a steady-state firing angle resonance that depends on the equipment's X_C/X_L ratio, as illustrated in Fig. 2a, which its discontinuity configures an unrealistic reactive power generation by the SVC.

The reactive power injected or absorbed by a SVC connected in a generic bus "k" which controls the voltage magnitude of a bus "m" is given by (11) [1, 4]. The aforementioned equation considers the SVC reactive power injected into the network to be positive.

$$X_{L_{\text{eq}}}(\alpha) = \frac{X_L \cdot \pi}{[2 \cdot (\pi - \alpha) + \sin(2\alpha)]} \tag{8}$$

$$X_{\text{eq}}(\alpha) = \frac{X_C \cdot X_L}{\frac{X_C}{\pi} \cdot [2 \cdot (\pi - \alpha) + \sin(2\alpha)] - X_L} \tag{9}$$

$$B_{\text{eq}}(\alpha) = -\frac{\frac{X_C}{\pi} \cdot [2 \cdot (\pi - \alpha) + \sin(2\alpha)] - X_L}{X_C \cdot X_L} \tag{10}$$

$$Q_{G_k} = V_k^2 \cdot B_{\text{eq}}(\alpha) \tag{11}$$

According to Fig. 2b, for values of α smaller than α^0 the equipment characteristic is inductive, whereas for values of α bigger than α^0, the characteristic is capacitive. This methodology [2], therefore, only defines two operational regions for the SVC which are separated by α^0 value, and is able to ideally control the voltage magnitude at reference value of a specified control bus "m" (characterizing a *droop* simplification). For the proposed illustrative example, the capacitive and inductive reactances are considered equal to 50 Ω and 25 Ω, respectively.

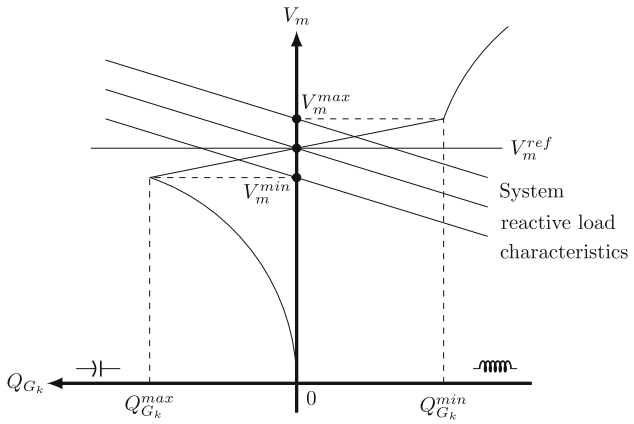

Fig. 3 SVC reactive power generation per voltage characteristic

3.2 SVC's reactive power injection methodology

In contrast to the thyristor firing angle methodology, the SVC's reactive power injection methodology is based on the equipment's controlled bus voltage magnitude per reactive power generation characteristic (QV-curve) illustrated in Fig. 3. In this methodology, the reactive power generated by the SVC is taken as the new state variable and, therefore, is no longer equivalent to Eq. (11).

Analyzing Fig. 3, three distinct operating regions are highlighted. The SVC capacitive operational region is superiorly delimited by the equipment's maximum reactive power value ($Q_{G_k}^{\max}$) and the controlled bus minimum voltage magnitude ($V_m^{\min}$). On the other hand, the inductive operational region is inferiorly delimited by the minimum reactive power value ($Q_{G_k}^{\min}$) and the controlled bus maximum voltage magnitude ($V_m^{\max}$). There is also a linear region, in between the capac-

itive and inductive regions, that is characterized by a *droop* which adjusts the SVC controlled bus voltage according to the network behavior, varying around a referenced value (V_m^{ref}).

In an ideal world, the linear operational region would not have *droop*, and the SVC would be able to control the voltage at a referenced value. However, as mentioned by [22], the *droop* must be considered in the SVC's modeling in order for current, susceptance, and reactive power vary accordingly, adopting to it values between 1% and 5%.

The *droop* variable is proposed to be implemented into the SVC's thyristor firing angle methodology, to improve the modeling of this device during power flow analysis.

4 Proposed methodologies

The proposed methodologies are incorporated into the traditional Newton–Raphson problem formulation (12) as described in Sect. 2, where the power equations and control equations are synthesized as follows:

$$\boldsymbol{f}(\boldsymbol{\theta}, \mathbf{V}, \boldsymbol{x}) = \mathbf{0} \tag{12}$$

For each control equation $\boldsymbol{y}$ considered in the power flow problem, it is employed a set of switches based on the sigmoid function equation defined in (13):

$$\text{sig}(x) = \frac{1}{1 + e^{-a \cdot (x - c)}} \tag{13}$$

where a represents the sigmoid function slope and c is the x-axis point where the inflection happens.

The smoothness is, therefore, introduced in function $\boldsymbol{f}$ by the employment of sigmoid switches with high slope values in control equations modeling. Although the adoption of high slope value approximates the sigmoid curve to a step curve, it avoids sigmoid function outputs different than 0 and 1. Therefore, the sigmoid function is able to eliminate the action of control equations models that are set to be inactive and consider only the action of the control equation model that should be active at the given operation state of the SVC. The so-called non-smooth transition between control equations is transformed into a smooth transition with the adoption of sigmoid functions.

The following subsections will detail the respective formulations proposed to model SVCs' reactive power generation. Firstly, the sigmoid switches will be employed to model the SVC reactive power injection model. Afterward, the sigmoid switches will be employed to propose a new SVC thyristor firing angle modeling based on the one developed by [2], proposing also an improvement to incorporate the *droop* variable into the model. At the end, a set of succinct observations comparing the proposed SVC models will be pointed out in Sect. 4.3.

Table 1 SVCs' sigmoid switches operation and control equation output

SVC operational region		sw1	sw2	Δy
1	Inductive	1	0	$\left(V_k^2 \cdot B_{\text{ind}} - Q_{G_k}\right)$
2	Linear	0	0	$\left(V_m^{\text{sch}} + r \cdot Q_{G_k} - V_m\right)$
3	Capacitive	0	1	$\left(V_k^2 \cdot B_{\text{cap}} - Q_{G_k}\right)$

4.1 SVCs' reactive power injection methodology

For this methodology, two sigmoid switches are employed to model SVCs reactive power generation. The switches are labeled sw1 and sw2, and their expressions are given by (14a) and (14b), respectively. Taking into account that the SVC purpose is to inject or absorb reactive power in order to control a specified bus voltage magnitude at a referenced value (V_m^{ref}), the switches are centered at $\lim_{\text{sup}}^{v}$ and $\lim_{\text{inf}}^{v}$, respectively.

$$\text{sw1} = \frac{1}{1 + e^{-slp \cdot (V_m - \lim_{\text{sup}}^{v})}} \tag{14a}$$

$$\text{sw2} = \frac{1}{1 + e^{+slp \cdot (V_m - \lim_{\text{inf}}^{v})}} \tag{14b}$$

where:

- $\lim_{\text{sup}}^{v}$ is equal to $\left(V_m^{\text{sch}} + r \cdot B_{\text{ind}} \cdot V_k^2\right) + tol^v$
- $\lim_{\text{inf}}^{v}$ is equal to $\left(V_m^{\text{sch}} + r \cdot B_{\text{cap}} \cdot V_k^2\right) - tol^v$

$$B_{\text{cap}} = B_{\max} = B(\alpha = 180°) = \frac{Q_{G_k}^{\max}}{\left(V_k^{\min}\right)^2} \tag{15}$$

$$B_{\text{ind}} = B_{\min} = B(\alpha = 90°) = \frac{Q_{G_k}^{\min}}{\left(V_k^{\max}\right)^2} \tag{16}$$

Combining the sigmoid switches with the SVC's operational regions equations, in (17) it is presented the control equation of the SVC taking Q_{G_k} as the new state variable to be updated at each iteration process.

$$\begin{aligned} y = {} & \text{sw1} \cdot \left(Q_{G_k} - V_k^2 \cdot B_{\text{ind}}\right) + \text{sw2} \cdot \left(Q_{G_k} - V_k^2 \cdot B_{\text{cap}}\right) \\ & + \left(1 - \text{sw1}\right) \cdot \left(1 - \text{sw2}\right) \cdot \left(V_m - V_m^{\text{sch}} - r \cdot Q_{G_k}\right) \end{aligned} \tag{17}$$

In accordance with (17), it is determined in Table 1 the control equation residue for each operational state of the SVC. It is worth noting that the condition on which both keys present high binary value is never achieved.

On account of the control equation (17) and consequently the new state variable, the Jacobian matrix shape is redefined.

A new line and new column will be appended to the original matrix formation for each SVC connected on the electrical system, as determined in (1).

4.2 SVCs' thyristor firing angle methodology

Differently to the previous methodology, four sigmoid switches are employed to model SVCs reactive power generation based on [2]. The switches are labeled $sw3$ through $sw6$, and their expressions are given by (18a) through (18d), respectively. Considering that the SVC reactive power generation depends on the equipment's thyristor firing angle, switches sw3 and sw4 are centered at $\lim^{\alpha}_{\max}$ and $\lim^{\alpha}_{\min}$, respectively. Accordingly, switches sw5 and sw6 refer to the controlled bus maximum and minimum voltage magnitude and are centered at $\lim^{v}_{\sup}$ and $\lim^{v}_{\inf}$.

$$\text{sw3} = \frac{1}{1 + e^{-\text{slp}\cdot(\alpha\ -\ \lim^{\alpha}_{\max})}} \tag{18a}$$

$$\text{sw5} = \frac{1}{1 + e^{-\text{slp}\cdot(V_m\ -\ \lim^{v}_{\sup})}} \tag{18b}$$

$$\text{sw4} = \frac{1}{1 + e^{+\text{slp}\cdot(\alpha\ -\ \lim^{\alpha}_{\min})}} \tag{18c}$$

$$\text{sw6} = \frac{1}{1 + e^{+\text{slp}\cdot(V_m\ -\ \lim^{v}_{\inf})}} \tag{18d}$$

where

- $\lim^{\alpha}_{\max}$ is equal to $180° - \text{tol}^{\alpha}$
- $\lim^{\alpha}_{\min}$ is equal to $90° + \text{tol}^{\alpha}$
- $\lim^{v}_{\sup}$ is equal to $\left(V^{\text{ref}}_m + r \cdot B_{\text{eq}}(90°) \cdot V^2_k\right) + \text{tol}^{v}$
- $\lim^{v}_{\inf}$ is equal to $\left(V^{\text{ref}}_m + r \cdot B_{\text{eq}}(180°) \cdot V^2_k\right) - \text{tol}^{v}$

These switches are used to design the control equation that models SVCs' reactive power generation and that will be added to the power flow nonlinear system of equations. The control equation takes α as the new state variable to be updated at each iteration process and is given by (19).

$$\begin{aligned} y\ &= \text{sw4} \cdot \text{sw5} \cdot \left(\alpha - 90°\right) + \text{sw3} \cdot \text{sw6} \cdot \left(\alpha - 180°\right) \\ &\quad + \big[\text{sw4} \cdot (1 - \text{sw5}) + \text{sw3} \cdot (1 - \text{sw6}) \\ &\quad + (1 - \text{sw4}) \cdot (1 - \text{sw5}) \cdot (1 - \text{sw3}) \cdot (1 - \text{sw6})\big] \cdot \\ &\quad \left(V_m - V^{\text{ref}}_m - r \cdot Q_{G_k}\right) \end{aligned} \tag{19}$$

where Q_{G_k} is given in (11).

In accordance with (19), it is determined in Table 2 the control equation residue for each operational states of the SVC. It is worth noting that the condition on which switches sw3 and sw4 present high binary value is never achieved. The same stands for switches sw5 and sw6.

Once more, the Jacobian matrix shape must be redefined, by which a new line and new column will be appended to the original matrix formation for each SVC connected on the electrical system, as determined in (1).

4.3 Observations on SVC methodologies

The *droop* implementation in the thyristor firing angle methodology is set clear in (19), where the *droop* variable "r" multiplies the terms of the reactive power variable Q_{G_k} given in (11). With this consideration, the improved thyristor firing angle methodology returns the same results as the reactive power injection methodology. In order to illustrate the *droop* implementation, Fig. 4 presents the SVC controlled bus voltage variation per reactive power generated and per thyristor firing angle.

In both figures, the SVC thyristor firing angle with 0% *droop* implementation refers to the methodology proposed by [2]. Although the SVC 0% *droop* model is able to control the bus voltage magnitude at the referenced value, this operation is in fact idealized and does not occur due to physical operational limitations of the equipment. By adopting other values for the *droop*, a more realistic operation by the control device is obtained [22].

For both methodologies, to avoid direct transition between inductive and capacitive regions, a step through the linear region is performed, equaling the controlled bus magnitude to its schedule value and the specified state variable to result in null reactive power by the SVC. For the thyristor firing angle methodology, if α is within limits when the controlled bus magnitude V_m violates one of its limits, then α value is fixed at V_m's corresponding limit.

5 Simulation results and discussion

The proposed methodologies for SVC's reactive power generations were applied in two systems. The first is a small-scale tutorial system [1]. The second is the well-known IEEE Nordic system [13], and a medium-scale network with more than 70 buses and 100 lines. As a evaluating tool, it is employed the power flow continuation method [24], which combines the power flow system of nonlinear equations (12) with a given increase on the system's loading parameter variable λ, as shown in (20).

$$\boldsymbol{f}(\boldsymbol{\theta}, \mathbf{V}, \boldsymbol{x}, \lambda) = 0 \tag{20}$$

Both systems were simulated in Python programming code and validated via the aforementioned production-grade

Table 2 SVCs' sigmoid switches operation and control equation output

SVC operational region		sw3	sw4	sw5	sw6	Δy
1	Inductive	0	1	1	0	$(90° - \alpha)$
2		0	1	0	0	
3	Linear	0	0	0	0	$\left(V_m^{\text{sch}} + r \cdot V_k^2 \cdot B_{\text{eq}}(\alpha) - V_m\right)$
4		1	0	0	0	
5	Capacitive	1	0	0	1	$(180° - \alpha)$

software. Since SVCs in the given software are modeled via reactive power injection methodology, only the SVC thyristor firing angle sigmoid methodology will be applied in Python simulations.

5.1 Tutorial system

This small-scale tutorial system represents a high-voltage network that is used in studies of power systems maximum loading condition [1]. The system topology along with the bus and line data is shown in Fig. 5.

For this system, the generator connected at Bus B_2 operates as a synchronous condenser. Analyzing the network behavior through power flow continuation, it is seen that Bus B_3 has the most critical voltage profile. Hence, the analysis of Bus B_3 voltage magnitude variation is proposed in respect of generator or SVC connected at Bus B_2, with simulations results being highlighted in Figs. 6 and 7, respectively. The continuous lines refer to the implementation of the proposed methodologies in Python, and the circles refer to the values obtained via the production-grade software.

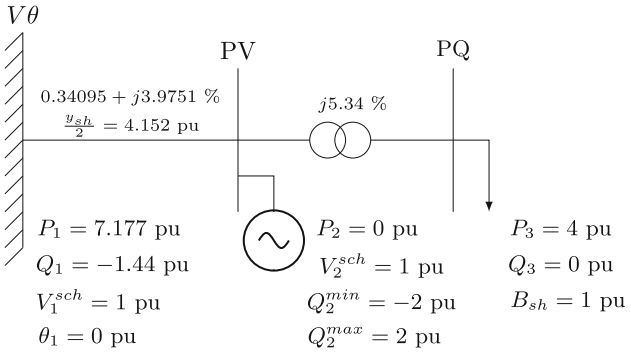

Fig. 5 Small-scale tutorial system topology. Adapted from [1, p. 968]

In Fig. 6, the orange line represents Bus B_3 voltage profile that is controlled by a synchronous condenser connected at Bus B_2. As it can be seen, the equipment is able of correctly controlling Bus B_3 voltage magnitude at the referenced value.

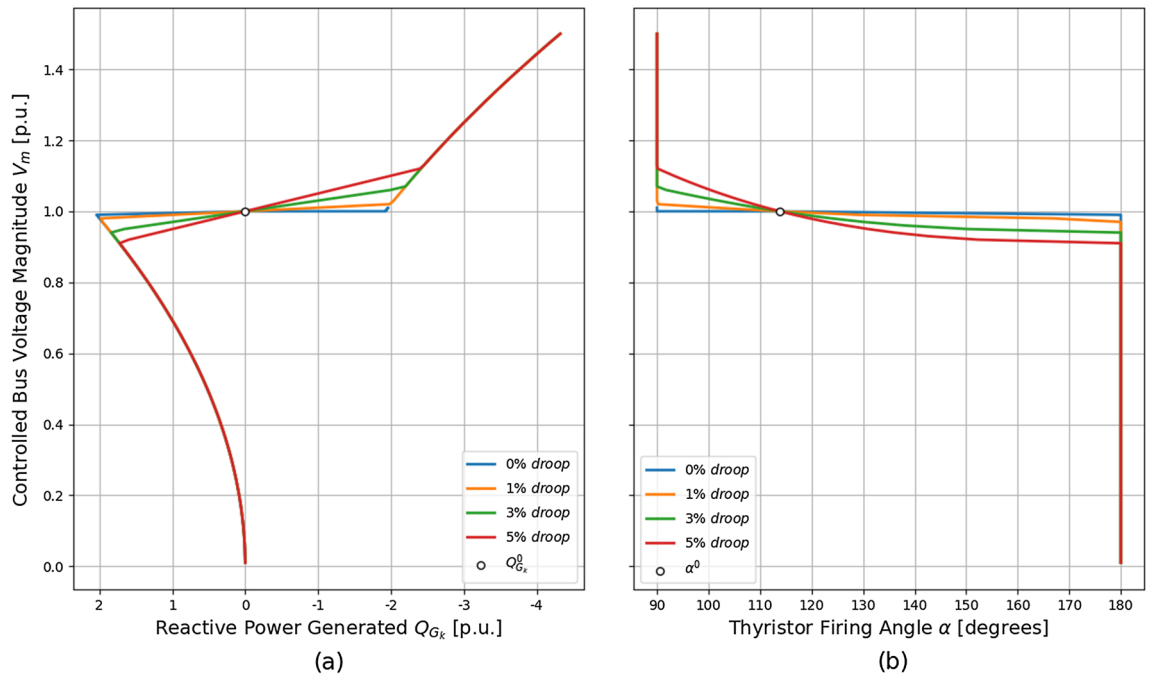

Fig. 4 SVC controlled bus voltage magnitude **a** per reactive power generated and **b** per thyristor firing angle

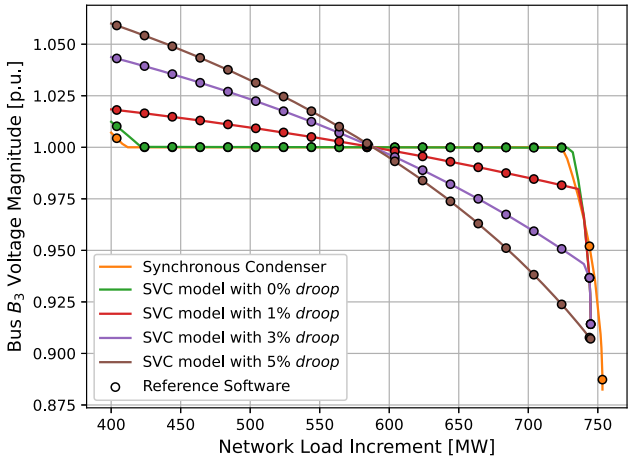

Fig. 6 Bus B_3 voltage magnitude variation by network load increment

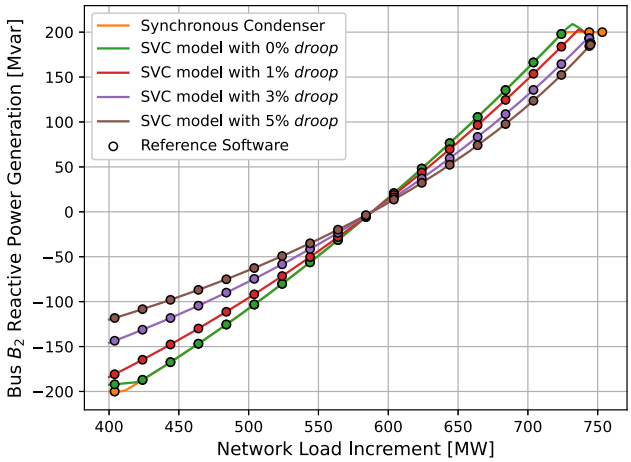

Fig. 7 Bus B_2 reactive power generation by network load increment

A similar voltage profile is depicted in the blue color, with the generator being substituted by a SVC with equal range of reactive power generation. In this analysis, the SVC is modeled without *droop* as proposed by [2] and is also able to control Bus B_3 voltage magnitude at the referenced value.

Despite the same results, it is observed that the synchronous condenser and SVC tend to vary in the nonlinear regions. The main reason to it is because the reactive power injected/absorbed by the synchronous condenser stays fixed at the violated limit, while the SVC, in turn, only the equivalent susceptance stays fixed at the corresponding limit ($\alpha = 90°$ or $\alpha = 180°$). This situation is better represented by (21), as pointed out by [2]:

$$Q_{G_k}^{\text{violated}} \neq B_{\text{eq}}^{\text{fixed}} \cdot V_k^2. \tag{21}$$

By applying different *droop* values to the SVC methodology, a better bus voltage magnitude profile is obtained which is closer to SVC realistic operation. In Fig. 6, the 1%, 3%, and 5% *droop* implementations in the SVC thyristor firing angle methodology can be seen in red, purple, and brown colors, respectively.

Consequently, each implemented methodology results in different reactive power generation profile as shown in Fig. 7. Within each profile, it is certified that the *droop* value weights on the reactive power generation in terms of the equipment's maximum or minimum generation limit. This situation indicates that, depending on the adopted *droop* value in the steady-state SVC model, the control device will have broader range of reactive power generation within the linear operational region until it reaches its limit.

Analyzing the tutorial system example, in Fig. 7, modeling the SVC with 5% *droop* gives the control device a broader range of reactive power generation within the linear operational region. Additionally, the characteristic highlighted in Eq. (21) is also depicted in Fig. 7, better emphasized by the synchronous condenser and SVC with 0% *droop* models.

5.2 Nordic system

Given the Nordic system topologies detailed in [13], in this paper only topology A will be studied. Hence, the Nordic system topology A is shown in Fig. 8, whereas the bus and line data are available at [13]. Analyzing the network behavior through continuation power flow [24], it is seen that Bus 1041 has the most critical voltage profile. Therefore, the aforementioned bus voltage magnitude control variation will be evaluated in respect of a generator or SVC connected to itself.

For this case, the continuation power flow simulation results are presented in Figs. 9 and 10. Figure 9 displays Bus 1041 voltage magnitude variation default condition, when there is no equipment connected, as well as for a synchronous condenser or SVC operating connected at the bus. As it can be seen, the presence of a synchronous condenser or SVC connected at Bus 1041 not only enhances its voltage magnitude profile, resulting in a smaller variation, but also contributes to a larger network load increment.

Similarly as discussed in Sect. 4.1, synchronous condenser and SVC with 0% *droop* models are able to maintain the voltage profile at the referenced value throughout most of the power flow continuation simulation. This operational condition, however, is acceptable only for generators since the *droop* between 1% and 5% must be taken into consideration into SVCs modeling [22]. Although each *droop* implementation value results in a different controlled bus voltage magnitude variation, the presence of SVC still enhances the voltage magnitude profile and provides an increase in system's load margin, as shown in Fig. 9.

On a further analysis, observing Fig. 9 along with Table 3, it is highlighted benefits that SVCs provide to the system in terms of loading margin and critical voltage magnitude parameters. If a minimum voltage magnitude limit is set at 0.95 p.u., for example, and simulating the continuous power

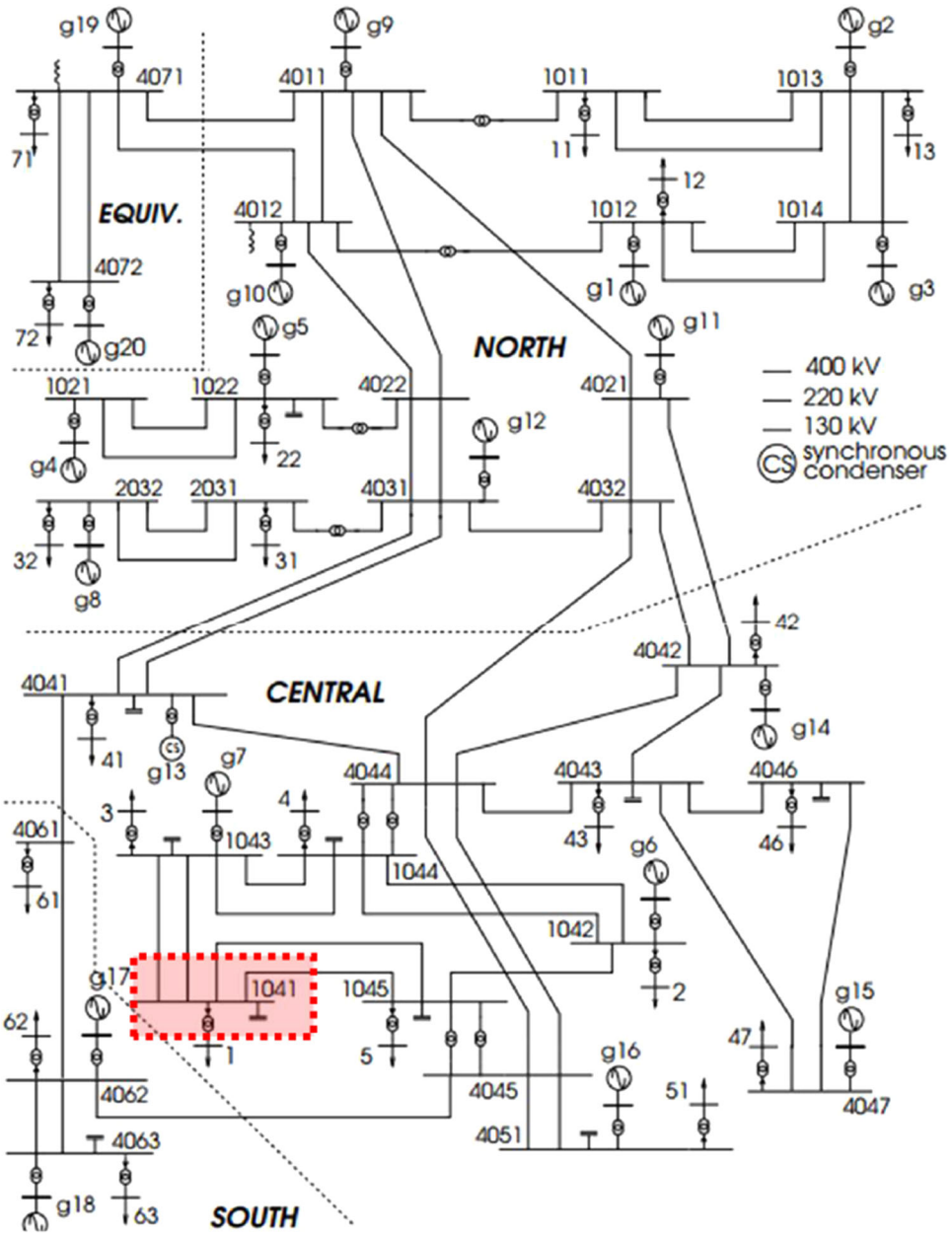

Fig. 8 IEEE Nordic system topology [13] highlighting Bus 1041 with the most critical voltage magnitude profile

flow for the desired system, differences on voltage magnitude profile are seen when a SVC is and is not connected to Bus 1041. Not only does the control device enhance the voltage magnitude for Bus 1041, but also does improve the system loading margin overall.

Considering the *droop* in the proposed methodologies, simulating the steady-state SVC model in the continuous power flow can help determining the best value to adopt to it. Taking into account loading margin and critical voltage magnitude as parameters and the given information in Fig. 9 and Table 3, it can be assured that modeling the SVC with 1% *droop* presents the best results. In sense of transmission system expansion problem, such benefits guaranteed by SVCs are translated into a more secure, resilient and stable operation condition for the power network.

It is worth noting that Fig. 10 illustrates the differences in the implementation of each droop value within the steady-state SVC model concerning the reactive power generation profile. It can also be noted the ranges of reactive power generation within the linear operational region until the limit is reached for the selected SVC *droop* values. Analyzing the Nordic system example, in Fig. 10, modeling the SVC with 5% *droop* gives the control device a broader range of reactive power generation within the linear operational region. For the proposed example, the control devices limits are $\pm$ 200 MVAr.

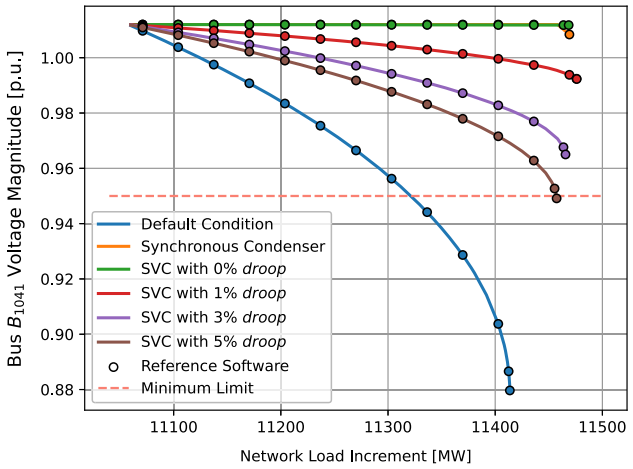

Fig. 9 Bus 1041 voltage magnitude variation by network load increment

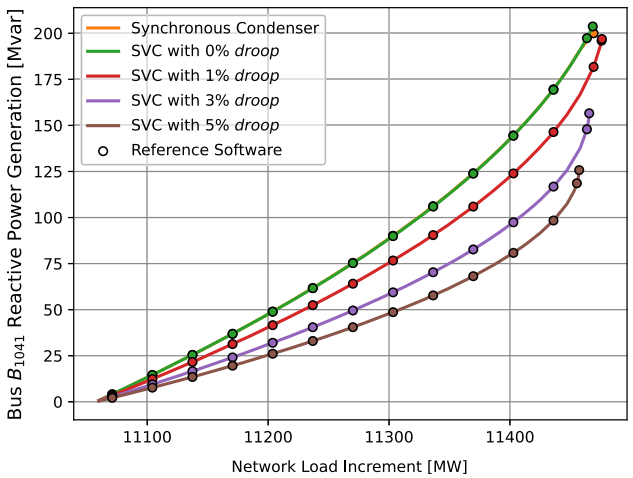

Fig. 10 Bus 1041 reactive power generation by network load increment

Table 3 Impacts of adopted *droop* values on SVC models

Parameters	Default	SVC *Droop*		
	condition	1%	3%	5%
Loading margin [MW]	265.44	416.07	405.65	397.36
Critical voltage magnitude[p.u.]	0.9485	0.9923	0.9646	0.9485

6 Conclusions

This paper has presented a review of the main methodologies as well as new techniques for modeling SVCs in the power flow problem. A contribution to the SVC thyristor firing angle methodology developed by [2] is also proposed, considering the voltage *droop* for the linear region of operation of the control device.

The implementation of sigmoid function-based switches contributes positively on the proposed representations. It was verified that the efficiency and accuracy of all proposed methodologies presented same precise results as those obtained via the reference software used in a significant fewer number of iterations.

In the modeling of SVCs, the sigmoid switches not only enable the insertion of the control device's exact control equation into the Jacobian Matrix, but also enable the correct transitions through the equipment's operational regions avoiding extra iterations. Additionally, the sigmoid switches avoid unnecessary bus-type re-specification during the power flow and continuous power flow simulations, even if a SVC's reactive power generation limit is reached.

Lastly, when comparing SVCs' thyristor firing angle methodology with the reactive power injection methodology, it was verified that the state variable α tends to be more sensitive than the state variable Q_{G_k}. This is reassured in Fig. 2b, in which small variations in α can provoke large variations in the equipment's equivalent susceptance and, consequently, in the reactive power generation. Both models, however, are appropriated for representing SVCs in the power flow problem efficiently, while the former is more indicated for those studies where the assessment of firing angles may be important.

Acknowledgements The authors would like to thank the National Research Council (CNPq), the State of Minas Gerais Research Foundation (FAPEMIG), and the Brazilian Federal Agency for Support and Evaluation of Graduate Education (CAPES).

Author Contributions JPPB and JAPF contributed to conceptualization, methodology, validation, formal analysis, investigation, resources, data curation, writing—original draft preparation, writing–review and editing, and visualization; JPPB provided software; JAPF was involved in supervision; and all authors have read and agreed to the published version of the manuscript.

Declarations

Conflict of interest The authors have no competing interests to declare that are relevant to the content of this article.

References

1. Kundur P (1994) Power system stability and control. McGraw-Hill, New York, p 1176
2. Ambriz-Perez H, Acha E, Fuerte-Esquivel CR (2000) Advanced svc models for Newton-Raphson load flow and newton optimal power flow studies. IEEE Trans Power Syst 15(1):129–136. https://doi.org/10.1109/59.852111
3. Perez M, Messina A, Fuerte-Esquivel C (2000) Application of facts devices to improve steady state voltage stability. In: 2000 power engineering society summer meeting (Cat. No. 00CH37134), vol. 2, pp. 1115–1120. IEEE
4. Miller TJE et al (1982) Reactive power control in electric systems, vol 2. Wiley, New York, New Jersey
5. Mahdad B (2020) Improvement optimal power flow solution considering SVC and TCSC controllers using new partitioned ant lion algorithm. Electr Eng 102(4):2655–2672

6. Mi Y, Ma C, Fu Y, Wang C, Wang P, Loh PC (2018) The svc additional adaptive voltage controller of isolated wind-diesel power system based on double sliding-mode optimal strategy. IEEE Trans Sustain Energy 9(1):24–34. https://doi.org/10.1109/TSTE.2017.2713700
7. Nepomuceno EG, Neto OM, Takahashi RHC, Tavares CE (2003) A heuristic approach to robust control design for power systems with several facts devices. Int J Electr Power Energy Syst 25(1):13–20. https://doi.org/10.1016/S0142-0615(02)00035-2
8. Rana AS, Bajaj M, Gairola S (2019) Optimal power flow solution in smart grid environment using SVC and TCSC. In: Ustun TS (ed) Advanced communication and control methods for future smartgrids. IntechOpen, Rijeka. https://doi.org/10.5772/intechopen.86113
9. Sekhar DAH, Haritha A, Vandana A, Teja PC (2020) Novel hybrid optimization techniques for analyzing the performance of transmission lines using SVC device. Int J Electr Eng Technol 11(1):1–14
10. Neves LS, Alberto LFC (2020) On the computation of the locally closest bifurcation point considering loading uncertainties and reactive power limits. IEEE Trans Power Syst 35(5):3885–3894
11. Neves LS, Alberto LFC, Chiang HD (2022) Smooth power flow model for unified voltage stability assessment: theory and computation. IEEE Trans Power Syst. https://doi.org/10.1109/TPWRS.2022.3145332
12. Gu W, Milano F, Jiang P, Tang G (2007) Hopf bifurcations induced by SVC controllers: a didactic example. Electr Power Syst Res 77(3):234–240
13. Van Cutsem T, Glavic M, Rosehart W, Santos J, Cañizares C, Kanatas M, Lima L, Milano F, Papangelis L, Andrade Ramos R et al (2015) Test systems for voltage stability analysis and security assessment. Technical report, IEEE
14. Tinney WF, Hart CE (1967) Power flow solution by Newton's method. IEEE Trans Power Appar Syst PAS–86(11):1449–1460. https://doi.org/10.1109/TPAS.1967.291823
15. Stott B (1974) Review of load-flow calculation methods. Proc IEEE 62(7):916–929. https://doi.org/10.1109/PROC.1974.9544
16. Maria GA, Yuen AH, Findlay JA (1988) Control variable adjustment in load flows. IEEE Trans Power Syst 3(3):858–864. https://doi.org/10.1109/59.14533
17. Santos MJ, Pereira JLR, Filho JAP, Oliveira EJ, Silva IC (2004) A new approach for area interchange control modeling. IEEE Trans Power Syst 19(3):1271–1276. https://doi.org/10.1109/TPWRS.2004.831289
18. Passos Filho JA, Martins N, Falcao DM (2009) Identifying power flow control infeasibilities in large-scale power system models. IEEE Trans Power Syst 24(1):86–95. https://doi.org/10.1109/TPWRS.2008.2009390
19. Zhao J, Chiang HD, Zhang BM (2005) Study on PV-PQ bus type switching logic in power flow computation. Proc CSEE 25(1):54–59
20. Pirnia M (2014) Stochastic modeling and analysis of power systems with intermittent energy sources. PhD thesis
21. Mathur RM, Varma RK (2002) Thyristor-based FACTS controllers for electrical transmission systems. John Wiley & Sons, New Jersey
22. Taylor CW, Scott G, Hammad A (1994) Static var compensator models for power flow and dynamic performance simulation. IEEE Trans Power Syst 9(1):229–240. https://doi.org/10.1109/59.317606
23. Erinmez IA (1986) Static var compensators. CIGRÉ Working Group 38-01, Task Force No. 2 on SVC
24. Ajjarapu V, Christy C (1992) The continuation power flow: a tool for steady state voltage stability analysis. IEEE Trans Power Syst 7(1):416–423. https://doi.org/10.1109/59.141737